Japan Geoscience Union Meeting 2012
(May 20-25 2012 at Makuhari, Chiba, Japan)

PCG33-01 Room:202 Time:May 25 09:00-09:15

Current status of Venus orbiter Akatsuki

NAKAMURA, Masato[1*], IMAMURA, Takeshi[1]

[1]Institute of Space and Astronautical Science, Japan Aerospace Exploration Agency

The first Venus probe of Japan, Akatsuki, was launched in May 2010. The Venus orbit insertion maneuver conducted in December 2010 has failed due to a malfunction of the propulsion system, and at present the spacecraft is orbiting the Sun. Akatsuki will have a chance to encounter Venus in 2015; the project team is examining the possibility of conducting an orbit insertion maneuver again at this opportunity.

Keywords: Venus, exploration, Akatsuki

Japan Geoscience Union Meeting 2012
(May 20-25 2012 at Makuhari, Chiba, Japan)

PCG33-02 Room:202 Time:May 25 09:15-09:30

Atmospheric structure in the cloud-top altitude region of Venus

TAGUCHI, Makoto[1*], FUKUHARA, Tetsuya[2], FUTAGUCHI, Masahiko[1], IMAMURA, Takeshi[3], NAKAMURA, Masato[3], UENO, Munetaka[3], IWAGAMI, Naomoto[4], SATO, Mitsuteru[2], MITSUYAMA, Kazuaki[4], HASHIMOTO, George[5]

[1]Rikkyo University, [2]Hokkaido University, [3]ISAS, [4]University of Tokyo, [5]Okayama University

The first Japanese Venus orbiter Akatsuki launched in May 2010 is a meteorological satellite which will reveals the 3-D structure of Venusian atmosphere using 5 cameras and a radio occultation experiment onboard. The Longwave Infrared Camera is one of the suite of cameras and measures thermal infrared radiation in the wavelength region of 8-12 um emitted from the cloud-top altitude region around 65 km. Observed data is converted to brightness temperature with absolute temperature accuracy of 3 K and noise-equivalent temperature difference of 0.3 K using an algorism developed by the pre-launch calibration experiment. Akatsuki arrived at Venus on December 7, 2010, but unfortunately the Venus orbit insertion was failed. While Akatsuki was traveling away from Venus, LIR acquired a few Venus images on December 9 and 10. The downloaded image is blurred because of spacecraft attitude change during the image acquisition. A clear image was obtained by precise correction of line-of-sight shift which is calculated from the brightness center position of Venus disk imaged in each intermediate image (Fig.1a).

The obtained brightness temperature maps show cloud-top temperature ranging from 225 to 240 K, the cold collar and dipole in the northern polar region, the limb darkening effect due to difference in optical depth versus zenith angle of line-of-sight, zonal structures and finer structures therein seen in the middle and low latitudes, and temporal variation of them. The observed limb darkening was reconstructed by a fitting calculation using model profiles of cloud optical depth and temperature. The retrieved optical depth exhibits a steep gradient at the upper cloud-top region and is 2-8 km lower in altitude than the initial profile. The brightness temperature map was corrected for the limb darkening effect thus calculated (Fig.1b), and compared with ultraviolet images obtained by the Venus Monitoring Camera (VMC) onboard Venus Express.

VMC observes solar light scattered by the cloud particles, while LIR observes thermal infrared radiation from the cloud particles. The light emitting altitude region is almost same for the UV and infrared images, though the observed hemisphere and local time are different. It is found that bright zonal belts exist in the latitude region of -45 to -55 both in the UV and mid-infrared images. This implies that the higher temperature belt where LIR can see deeper through the upper cloud with thin optical depth is laid in the latitude region where density of UV absorber is thin. The fact that the zonal structure extends for all local time suggests the cloud particles seen in the mid-infrared or the UV absorber can live longer than a few days. The mid-infrared images obtained by LIR show the brightness temperature distribution on the almost whole Venus nightside for the first time, and the information retrieved from the images gives constraint on the atmospheric dynamics and cloud chemistry in the cloud-top altitude region of Venusian atmosphere.

References

Taguchi et al., Icarus, in press, 10.1016/j.icarus.2012.01.024, 2012.

Figure 1. Brightness temperature distributions composited from 32 intermediate images (M=32 and N=32) (a) before and (b) after correction for the limb darkening effect. The illustration in the lower right shows equi-latitude and -longitude lines every 30 degree and the sunlit region of the Venus disk [Taguchi et al., 2012].

PCG33-02 Room:202 Time:May 25 09:15-09:30

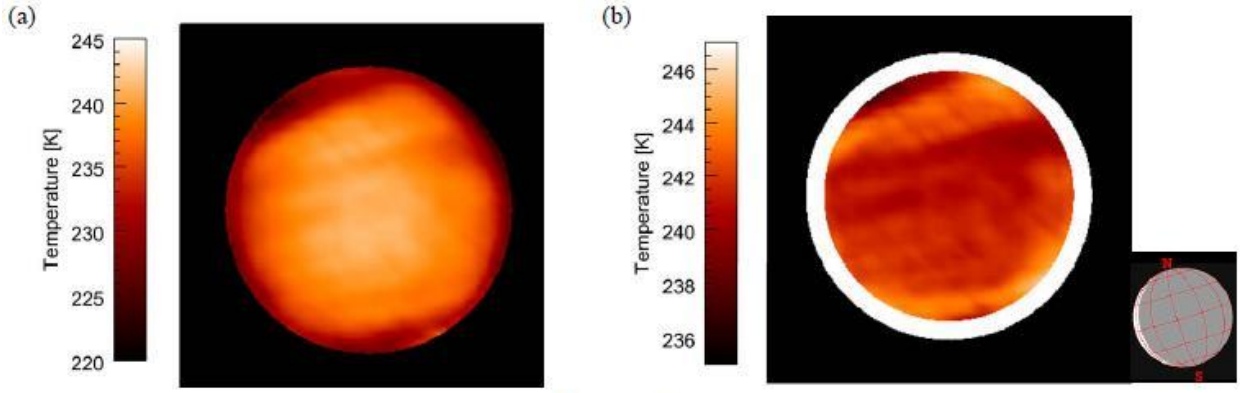

Figure 1

Japan Geoscience Union Meeting 2012
(May 20-25 2012 at Makuhari, Chiba, Japan)

PCG33-03 Room:202 Time:May 25 09:30-09:45

Venus' clouds as inferred from the phase curves acquired by IR1 and IR2 on board Akatsuki

SATOH, Takehiko[1*], OHTSUKI, Shoko[1], IWAGAMI, Naomoto[2], UENO, Munetaka[1], Kazunori Uemizu[1], SUZUKI, Makoto[1], HASHIMOTO, George[3], SAKANOI, Takeshi[4], KASABA, Yasumasa[4], NAKAMURA, Ryosuke[5], IMAMURA, Takeshi[1], NAKAMURA, Masato[1], FUKUHARA, Tetsuya[6], YAMAZAKI, Atsushi[1], YAMADA, Manabu[1]

[1]Japan Aerospace Exploration Agency, [2]University of Tokyo, [3]Okayama University, [4]Tohoku University, [5]National Institute of Advanced Industrial Science and Technology, [6]Hokkaido University

We present phase curves for Venus in the 1-2 micron wavelength region, acquired with IR1 and IR2 on board Akatsuki (February - March 2011). A large discrepancy with the previously-published curves was found in the small phase angle range (0^o - 30^o). Through analysis by radiative-transfer computation, it was found that the visibility of larger (˜1 micron or larger) cloud particles was significantly higher than in the standard cloud model. Although the cause is unknown, this may be related to the recently reported increase in the abundance of SO_2 in the upper atmosphere. It was also found that the cloud top is located at ˜75 km and that 1-micron particles exist above the cloud, both of these results being consistent with recent studies based on the Venus Express observations in 2006 - 2008. Further monitoring, including photometry for phase curves, polarimetry for aerosol properties, spectroscopy for SO_2 abundance, and cloud opacity measurements in the near-infrared windows, is required in order to understand the mechanism of this large-scale change.

Keywords: Venus, phase curve, cloud structure, Akatsuki, IR1, IR2

Japan Geoscience Union Meeting 2012
(May 20-25 2012 at Makuhari, Chiba, Japan)

PCG33-04 Room:202 Time:May 25 09:45-10:00

Vertical propagation and wind speed acceleration of planetary-scale waves at the cloud level of Venus

KOUYAMA, Toru[1*], IMAMURA, Takeshi[2], NAKAMURA, Masato[2], SATOH, Takehiko[2], Futaana Yoshifumi[3]

[1]University of Tokyo, [2]ISAS/JAXA, [3]Swedish Institute of Space Physics

In this study, we reveal temporal variation of the super-rotation of Venus atmosphere and spatial structures of planetary scale atmospheric waves at the cloud top level by deriving wind speeds and their variations at the cloud top from UV (365 nm) images taken by Venus Monitoring Camera (VMC) onboard Venus Express of European Space Agency. Because VMC has taken many cloud images covering from low to high latitudes of the southern hemisphere, well suited for derivation off wind speeds and their variations. We applied a newly-developed cloud tracking method (Ogohara et al., 2012; Kouyama et al., 2012) to these images and found that the equatorial zonal wind speed changes quasi-periodically, alternating ”fast season” (over 100 m s^{-1}) and ”slow season” (below 90 m s^{-1}) every ˜100 earth days.

From spectral analysis of the wind speed and the cloud brightness variations, planetary-scale 5 day period variations were identified in the zonal and meridional wind speeds in the fast season of background zonal wind speeds. The phase speed of the 5-day period variations is slower than the background wind speed. The phase relationship between the zonal and meridional winds implies that the 5-day variation is a manifestation of a Rossby wave. On the other hand, planetary-scale 4 day period variations were identified in zonal wind speeds and cloud brightness in the slow season. The phase speed of the 4-day period variations is faster than the background wind speed. These results are consistent with previous studies from Pioneer Venus observations (Del Genio and Rossow, 1990; Rossow et al., 1990).

From the numerical results based on Covey & Schubert (1982), we found that the Kelvin wave originating from the lower atmosphere can propagate vertically into the cloud top level in the slow period. On the other hand, the Rossby wave can propgate in the fast period. Therefore, the time variation of the super-rotation could be affected by these waves. In this study, we will evaluate the angular momentum transport by these waves based on the derived parameters from our analysis.

Keywords: Venus, super-rotation, atmospheric waves

Japan Geoscience Union Meeting 2012
(May 20-25 2012 at Makuhari, Chiba, Japan)

PCG33-05 Room:202 Time:May 25 10:00-10:15

Investigation of the HDO/H2O ratio in the Venus atmosphere from comparison with SOIR on board Venus Express

MATSUI, Hiroki[1*], IWAGAMI, Naomoto[1]

[1]University of Tokyo

By using the IRTF 3 m telescope in Hawaii in 2010, we obtained a disk-averaged HDO mixing ratio of 0.22 +/- 0.03 ppm for a representative height of 62-67 km. Based on previous H2O measurements, the HDO/H2O ratio there is found to be 140 +/- 20 times larger than the telluric ratio. This lies in between the ratios of 120 +/- 40 and 240 +/- 25, respectively, reported for the 30-40 km region (de Bergh et al. 1991) by ground-based night-side spectroscopy and for the 80-100 km region by solar occultation measurement on board the Venus Express (Fedorova et al. 2008). However, such a large difference between the 62-67 km and 80-100 km regions might be latitudinal not vertical origin because of localization of VEx data mostly at high latitudes. In addition, the measurement by Krasnopolsky (2010) in the evening at an altitude of 70 km shows a latitudinal structure showing an equatorial minimum. This is inconsistent to our measurements.

By examining measurements by SOIR on board Venus Express at the terminator, we tried to check the consistency with our data set, and succeeded to confirm larger D/H ratio at higher altitude with little latitudinal gradient although the D/H ratio seems to be very variable.

Fedorova A. et al. JGR 113 E00B22 2008
Krasnopolsky A. Icarus 209 314-322 2010
de Bergh et al. Science 251 547-549 1991

Keywords: Venus, HDO, spectroscopy, D/H ratio

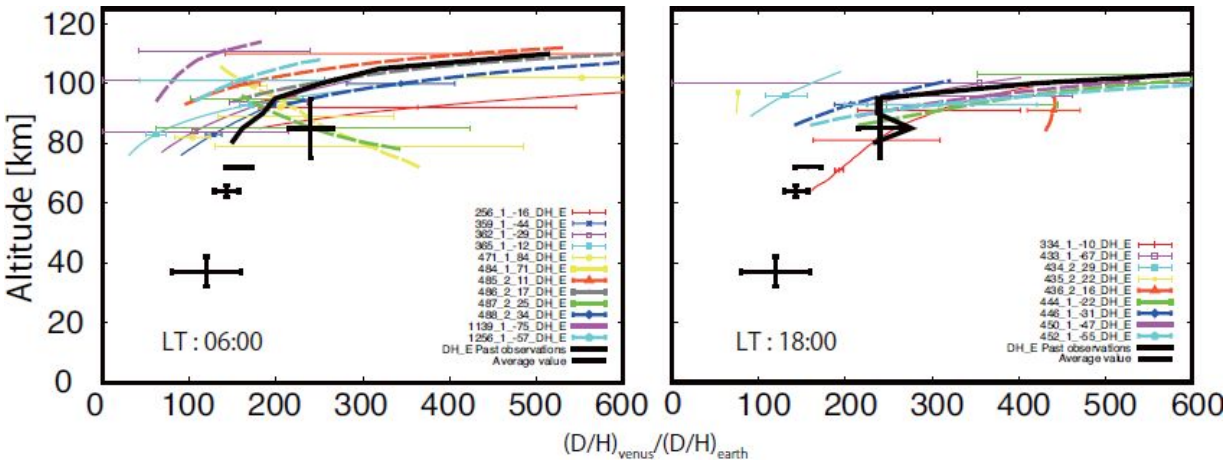

Japan Geoscience Union Meeting 2012
(May 20-25 2012 at Makuhari, Chiba, Japan)

PCG33-06 Room:202 Time:May 25 10:45-11:00

Evidence of ion acceleration by the local convection electric field: Venus Express observations

MASUNAGA, Kei[1*], FUTAANA, Yoshifumi[2], YAMAUCHI Masatoshi[2], TERADA, Naoki[1], OKANO, Shoichi[1]

[1]Grad. Sch. of Sci., Tohoku Univ., [2]Swedish Institute of Space Physics

Venus has no intrinsic magnetic field, so its upper atmosphere is directly exposed to the solar wind creating direct interactions between them. As a result of the interaction, ionospheric ions are removed from Venus mainly as O+. It is thought that the escaping oxygen from the atmosphere has played an important role in the atmospheric evolution on Venus. Pioneer Venus Orbiter and Venus Express have investigated the plasma environment of Venus. Many authors reported that high energy planetary oxygen ions were observed in the hemisphere to which a global convection electric field (Esw = -Vsw x Bsw) directs [e.g., Intriligator, 1989, Slavin et al., 1989; Barabash et al., 2007]. Thus, the convection electric field has been considered as a possible mechanism for the acceleration of planetary ions.

However, recently Masunaga et al., [2011] reported that a spatial distribution of outflowing O+ ions is strongly controlled by the IMF directions. By investigating two cases, IMF directs nearly perpendicular to the Venus-Sun line (perpendicular IMF case) and IMF directs nearly parallel to it (parallel IMF case), they indicated that the O+ ion acceleration mechanisms would be different. In the perpendicular IMF case, O+ fluxes are observed near the magnetic poles and x-component of the magnetic field reverses once per orbit. Sometimes the O+ flux is associated with the Bx reversal. Energy of those fluxes depends on the global convection electric field, which is consistent with previous studies [e.g. Intriligator, 1989; Slavin et al., 1989; Barabash et al., 2007]. These results can be understood by draping of the IMF around the Venus ionosphere followed by forming a single plasma sheet, and thus most of O+ ions are accelerated by the convection electric field and outflow through the plasma sheet. On the other hand in the parallel IMF case, a spatial distribution of O+ is different from that of the perpendicular IMF case. O+ fluxes are observed regardless of the convection electric field direction and Bx reverses multiple times per orbit. The fluxes are sometimes associated with the Bx reversal. Energy of the fluxes does not depend on the direction of the global magnetic field. This indicates that IMF drapes around the ionosphere more complicatedly and forms multiple outflow channels around the terminator. The independency of the outflow channel and the convection electric field direction indicates that O+ ions are not accelerated by the convection electric field but by local effects, such as a j x B force [Dubinin et al., 1993], viscous force [Perez-de-Tejada, 1997] or local convection electric field (EL = -VL x BL; where VL and BL is the local velocity vector and the local magnetic field).

In this study we concentrate on the effect of the local convection electric field and discuss whether or not the local electric field can explain the O+ acceleration observed by Venus Express. We show several examples to investigate dependence of oxygen ions' flow direction on the local convection electric field's direction by comparing with the global convection electric field's direction. The dependence between the O+ velocity vector and the local convection electric field is clearer than that on the global convection electric field in both cases. This may imply that planetary O+ ions could be accelerated by the local convection electric field.

References

Barabash et al., [2007], Nature, 450, 650-653, doi:10.1038/nature06434.
Dubinin et al., [1993], JGR, 98, A3, 3991-3997
Intriligator, [1989], GRL, 16, 2, 167-170
Masunaga et al., [2011], JGR, 116, A09326
Perez-de-Tejada, JGR, 106, A1, 211-219, 2001
Slavin et al., [1989], JGR, 94, A3, 2383-2398

Keywords: Venus, ASPERA, outflow, escape

Japan Geoscience Union Meeting 2012
(May 20-25 2012 at Makuhari, Chiba, Japan)

PCG33-07 Room:202 Time:May 25 11:00-11:15

Effects of the solar wind electric field on heavy-ion precipitation onto the Martian atmosphere: A statistical survey

HARA, Takuya[1*], SEKI, Kanako[1], FUTAANA, Yoshifumi[2], YAMAUCHI Masatoshi[2], BARABASH Stas[2], FEDOROV Andrei[3]

[1]STEL, Nagoya Univ., [2]IRF, Kiruna, Sweden, [3]CESR, Toulouse, France

The solar wind can directly interact with the Martian upper atmosphere, since Mars does not possess a global intrinsic magnetic field [e.g., *Acuna et al*., 1998]. Atmospheric escape phenomena induced by the solar wind interaction have been observed by Phobos-2 at solar maximum, and recently by Mars Express (MEX) at solar minimum [e.g., *Lundin et al*., 1989; *Barabash et al*., 2007]. Escape rates of planetary ions estimated by both spacecraft indicate a large dependence on the solar wind conditions [e.g., *Barabash et al*., 2007; *Lundin et al*., 2008]. It has been known that escaping planetary ions, which are picked up by interplanetary magnetic field (IMF) in the solar wind, are distributed highly asymmetrically in terms of the convective electric field [*Barabash et al*., 2007]. In addition to escaping ions, ions precipitating onto the Martian upper atmosphere should also contribute to atmospheric escape because they collide with atmospheric neutral particles, giving some particles sufficient energy to escape the planet [e.g., *Luhmann et al*., 1992]. This process is referred as ion sputtering. Ion sputtering could have been a significant escape process for ancient Mars due to the extreme solar EUV radiation, according to some results of numerical simulations [e.g., *Luhmann et al*., 1992; *Leblanc and Johnson*, 2002]. However, there are no conclusive in situ measurements of sputtering for Mars.

Precipitating planetary heavy ions with energies of up to a few keV were observed by MEX predominantly during CIR passages [*Hara et al*., 2011]. *Hara et al*., [2011] suggested that the flux of precipitating heavy ions is enhanced during CIR events because the gyroradius of picked-up ions is decreased to values comparable to the radius of Mars by the compressed IMF. The direction of the convective electric field in the solar wind should also be important for the behavior of picked-up ions. However, MEX does not carry any magnetic or electric field detectors, and therefore we cannot easily obtain the direction of the magnetic field or that of convective electric field in the solar wind.

Here we attempt to estimate the IMF orientation from MEX ion observations using the ring-like velocity distribution functions of picked-up protons of the exospheric origin [*Yamauchi et al*., 2006, 2008]. We are able to calculate the IMF orientation from the assumption that the gyration plane of these ions in velocity space is perpendicular to the IMF direction. Then, we conduct simple statistical trajectory tracings of picked up protons in physical space in order to determine the polarity of the IMF. We assume two IMF configurations (differing only in polarity) and traced a number of pickup protons. Then we can determine the polarity of IMF by inspecting which configuration better matches the observation. We also discuss the application of this method to statistically study effects of the solar wind electric field on the heavy-ion precipitation for Mars using the events in which both ring-ions and precipitating heavy ions are observed by MEX in the same orbit.

References:
Acuna, M. H., et al. (1998), *Science*, *279*, 1676–1680.
Barabash, S., et al. (2007), *Science*, *315*, 501–503.
Hara, T., et al. (2011), *J. Geophys. Res.*, *116*, A02309, doi:10.1029/2010JA015778.
Leblanc, F. and R. E. Johnson (2002), *J. Geophys. Res.*, *107*(E2), 5010.
Luhmann, J. G., et al. (1992), *Geophys. Res. Lett.*, 19(21), 2151–2154.
Lundin, R., et al. (1989), *Nature*, *341*, 609–612.
Lundin, R., et al. (2008), *Geophys. Res. Lett.*, *35*, L18203.
Yamauchi, M., et al. (2006), *Space Sci. Rev.*, *126*, 239–266.
Yamauchi, M., et al. (2008), *Planet. Space Sci.*, *56*, 1145–1154.

Keywords: Mars, Solar wind interaction, Atmospheric escape, Nonmagnetized planet

Japan Geoscience Union Meeting 2012
(May 20-25 2012 at Makuhari, Chiba, Japan)

PCG33-08 Room:202 Time:May 25 11:15-11:30

Three dimensional Mars' exosphere : multi-species thermal and nonthermal models

YAGI, Manabu[1*], Francois Leblanc[2], Jean-Yves Chaufray[2], Ronan Modolo[2], Sebastien Hess[2], Francisco Gonzalez-Galindo[3]

[1]STEL, Nagoya University, [2]LATMOS/IPSL, CNRS, France, [3]IAA-CSIC, Granada, Spain

The escaping rate of Mars' atmosphere is an important issue for its evolution. However, to know the atmospheric escape, it is crucial to well describe Mars' upper atmosphere and exosphere. In this presentation, a three dimensional exospheric model of the main constituents of Mars' thermosphere will be presented. This model describes the Martian exosphere as composed of thermal and non-thermal components. The thermal components of the O and CO2 exospheres are computed from a modified Chamberlain approach which is extended to three dimension including planetary rotation. A Monte Carlo test particle scheme is used to simulate the nonthermal O exosphere produced by dissociative recombination (DR) of O2+ in the thermosphere. The thermospheric and ionospheric conditions are calculated by Mars Global Circulation Model (Gonzalez-Galindo et al., Journal of Geophysical Research, 114, 2009). In this presentation, we will present the main results of this work (Yagi et al., Icarus, Submitted, 2012), that is, the seasonal variations of Mars' exosphere and of the atmospheric escape. This work is part of a project named HELIOSARES aiming to describe Mars' interaction with the solar wind by coupling different numerical models.

Keywords: Mars, Exosphere, Atmospheric Escaping, Simulation

Japan Geoscience Union Meeting 2012
(May 20-25 2012 at Makuhari, Chiba, Japan)

PCG33-09 Room:202 Time:May 25 11:30-11:45

Long-term variability of Na density in Mercury's atmosphere

DAIROKU, Hayato[1*], KAMEDA, Shingo[1], FUSEGAWA, Ayaka[1], KAGITANI, Masato[2], OKANO, Shoichi[2]

[1]Rikkyo University, [2]Tohoku University

Mercury has a very thin atmosphere. Its density is only a trillionth that of Earth's atmosphere; therefore, atoms and molecules in Mercury's atmosphere rarely collide. Hence, its atmosphere is called surface bounded exosphere. Atmospheric particles last only for short duration of a few hours in Mercury's atmosphere, indicating that sources of each of the constituents must exist on the planet. Mariner 10 detected H, He, and O, in Mercury's atmosphere; further, Na, K, and Ca were detected by ground-based observations. Atoms of these, Na haves ever been made ground-based observations. The three dominant source processes of Na atoms in Mercury's atmosphere are as follows.

1.Solar photon hitting the dayside surface of Mercury, Na atoms contained in the material surface are stimulated and emission.
2.Solar wind and ions in the magnetosphere hitting the surface of Mercury, and Na atoms get sputtered from the material surface.
3.Na atom emission for vaporization when the interplanetary dust on the ecliptic plane hit the surface of Mercury.

However, the most dominant among the abovementioned processes is yet to be clarified. Because of Mercury's proximity to the sun, observations cannot be made from about 30 min before sunrise or after sunset. This makes it impossible to study long-term (more than 1 h) variability of atmospheric density in order to determine the source of Na atoms. We conducted continuous spectroscopic observations of Mercury's exosphere with a 40-cm telescope at Haleakala Observatory in Maui. And we successed observation for 10 h during the daytime by replace the hood on the telescope to prevent stray light from hitting the primary mirror directly.

We compared the long-term variability of Na density in Mercury's atmosphere with date on the amount of solar wind particles such as ions and electrons around the planet; this data was obtained from NASA's MESSENGER spacecraft. We suggested a correlative relationship between the solar wind particles and the source processes of Na atoms in Mercury's atmosphere.

Keywords: Mercury, Na, airglow, Ground-based observation, Planetary Atmosphere, MESSENGER

Japan Geoscience Union Meeting 2012
(May 20-25 2012 at Makuhari, Chiba, Japan)

PCG33-10 Room:202 Time:May 25 11:45-12:00

MHD simulation of Kronian magnetosphere with the high resolution solar wind data

FUKAZAWA, Keiichiro[1*], Raymond J. Walker[2], Stefan Eriksson[3]

[1]Research Institute for Information Technology, Kyushu University, [2]IGPP/UCLA, [3]Laboratory for Atmospheric and Space Physics University of Colorado

In a series of studies we have reported that vortices formed at Saturn's dawn magnetopause in simulations when IMF was northward. We interpreted these vortices as resulting from the Kelvin Helmholtz (K-H) instability. Recently thanks to the developments of in computer performance and numerical calculation techniques, we have been able to perform the global magnetospheric simulations of the magnetosphere with much higher resolution than was previously possible. In these simulations we had sufficient resolution to model the signature of the field-aligned currents from the K-H vortices in Saturn's auroral ionosphere and found small patchy regions of upward field-aligned current which may be related to auroral emissions. Recently, patchy aurorae resembling our results have been reported from Cassini observations.

As a follow on study we have used Cassini observations of the solar wind upstream of Saturn to drive a simulation. Using these solar wind data we simulated the Kronian magnetosphere from 2008-02-12/14:00:31 to 2008-02-13/01:59:31. This simulation required about 1500 hours from 768 processor cores on a 10 TFlops supercomputer system with 1TB memory. Thus in this paper we will show the initial simulation results from the solar wind driven simulation and the configurations of vortices and aurorae at Saturn.

Japan Geoscience Union Meeting 2012
(May 20-25 2012 at Makuhari, Chiba, Japan)

PCG33-11 Room:202 Time:May 25 13:45-14:00

Scattering Properties of Jovian Aerosols from the Cassini ISS Limb-Darkening Observatioins

SATO, Takao M.[1*], SATOH, Takehiko[2], KASABA, Yasumasa[1]

[1]Department of Geophysics, Graduate School of Science, Tohoku University, [2]Institute of Space and Astronautical Science, Japan Aerospace Exploration Agency

This study provides new observational constraints on the scattering properties of aerosols in the Jovian upper troposphere and stratosphere. To achieve this objectives, we have analyzed imaging data during the Cassini flyby of Jupiter (October 2000-March 2001, solar phase angle coverage: 0-140 degrees) by utilizing its onboard Imaging Science Subsystem (ISS).

In this study, we present the analysis results of four sets of limb-darkening curves extracted along a bright zone (STrZ) and a dark belt (SEBn) from Jovian images in CB2 (750 nm) and BL1 (455 nm). To explain the solar phase angle behaviors of limb-darkening curves for each data set, we perform the radiative transfer calculations with a simple cloud model and the Mie theory applied to scattering of aerosols.

From these calculations, we find two important characteristics of cloud particles. One is the effective radius of cloud ($r_{eff,cloud}$). The best-fit $r_{eff,cloud}$ is obtained at 0.3 micron in CB2 and 0.2 micron in BL1. These values are in good agreement with those inferred from previous studies for the diffuse and ubiquitous layer of small particles in the upper troposphere as described in the synthesis works by West et al. (1986, 2004). The other is the real part of the refractive index of cloud ($n_{r,cloud}$). The best-fit $n_{r,cloud}$ for all data sets except for one data set ($n_{r,cloud}$ = 1.8) get a same value ($n_{r,cloud}$ = 1.85). Such values of $n_{r,cloud}$ are found to be much higher than previous experimental values of n_r for NH_3 ice particles (n_r ~ 1.4). Thus, we conclude that the best-fit combination of $n_{r,cloud}$ and $r_{eff,cloud}$ would strongly suggest the idea that the abundant small particle population in the upper troposphere is not composed of pure NH_3 ice. What actually eliminates the spectral signature of NH_3 ice around the 3-micron wavelength, despite the fact that significant depletion of NH_3 vapor has been observed for pressure levels of visible cloud layer, is unclear at this moment. The high real refractive index obtained in this study may hint at the composition of cloud particles for further studies.

As described above, the scattering properties of cloud particles for both the STrZ and the SEBn are found to show much the same characteristics, which suggests that the cloud particles themselves are less likely to be related to the visual difference between the zones and belts. We find that only the single scattering albedo of cloud shows a remarkable difference between two regions (this parameter gets a higher value for the STrZ than one for the SEBn), and is one key parameter which causes the visual difference. Our results support the idea proposed by West et al. (1986). Such difference in absorption would be likely to be due to chromophores (unknown coloring agents).

On the basis of these results, we compare our best-fit Mie phase functions for clouds obtained from all data sets with the phase functions derived by Tomasko et al. (1978) from the Pioneer 10 observations. The overall shapes of our Mie phase functions are found to be much flatter than those of their functions. Our Mie phase functions can reproduce the Pioneer 10 observations well. In contrast, Tomasko et al.'s function does not reproduce the Cassini observations. This is attributed to the fact that their phase function is under-constrained, primarily due to a considerable gap in observations for an intermediate solar phase angle (34-109 degrees).

A set of our new Mie phase functions has two advantages over Tomasko et al.'s functions:

1. since the Cassini data do not have a large gap in solar phase angle, the new Mie phase functions are better constrained;
2. the Mie phase function can easily be applied to different wavelengths.

With such characteristics, we now have a set of reliable baseline phase functions that can be used to interpret the ever-changing appearance of Jovian clouds as changes of the vertical cloud structure and/or distribution of chromophores in the atmosphere.

Keywords: Jupiter, atmosphere, aerosol, Cassini, radiative transfer

Japan Geoscience Union Meeting 2012
(May 20-25 2012 at Makuhari, Chiba, Japan)

PCG33-12 Room:202 Time:May 25 14:00-14:15

Ground-based telescope observation of Jupiter’s polar haze

OZAKI, Akihito[1*], TAKAHASHI, Yukihiro[1], Makoto watanabe[1], WATANABE, Shigeto[1], FUKUHARA, Tetsuya[1], SATO, Mitsuteru[1]

[1]Department of Cosmosciences, Graduate School of Science, Hokkaido University

It is known that Jupiter’s polar areas have haze which consists of aerosol particles and gas over which the sun-light is scattered. Haze is located in the layer higher than the cloud top so that the scattered light at the deep methane absorption line of 889 nm is much brighter than non-haze area. Horizontal haze structure is seldom investigated.

In this study, imaging observation of Jupiter’s polar haze used ground-based 1.6 m reflector named Pirka telescope operated by Hokkaido University. In order to investigate the temporal variation of the structure of the polar haze, image slices of the Jupiter at 889 nm at latitude of 67 degree, the low latitude edge of the polar haze region, are made for the data obtained in the period of 14:00 - 19:00 UT on 29 October 2011 and 10:30 - 15:00 UT on 31 October 2011. It is found that the polar haze has undulating pattern at the low latitude edge of polar haze like as Cassini observation in 2000, but the specific structures are different.

Keywords: Jupiter

Japan Geoscience Union Meeting 2012
(May 20-25 2012 at Makuhari, Chiba, Japan)

PCG33-13 Room:202 Time:May 25 14:15-14:30

Effect of the solar UV/EUV heating on the intensity and spatial distribution of Jupiter's synchrotron radiation

KITA, Hajime[1*], MISAWA, Hiroaki[1], TSUCHIYA, Fuminori[1], TAO, Chihiro[2], MORIOKA, Akira[1]

[1]Planetary Plasma and Atmospheric Research Center, Tohoku University, [2]ISAS/JAXA

Jupiter's synchrotron radiation (JSR) is the emission from relativistic electrons in the strong magnetic field of the inner magnetosphere, and it is the most effective probe for remote sensing of Jupiter's radiation belt from the Earth. Recent intensive observations for JSR reveal short term variations of JSR with the time scale of days to weeks. Brice and McDonough (1973) proposed a scenario for the short term variations (hereafter the B-M scenario); i.e, the solar UV/EUV heating for Jupiter's upper atmosphere drives neutral wind perturbations and then the induced dynamo electric field leads to enhancement of radial diffusion. If such a process occurs at Jupiter, brightness distribution of JSR is also expected to change. That is, it is expected that the dynamo electric field induced by diurnal neutral wind system produces dawn-dusk electric potential difference and dawn-dusk asymmetry in electron spatial distribution. Then, this makes dawn-dusk asymmetry of the JSR brightness distribution.

Preceding studies confirmed the existence of the short term variations in total flux density and its variation corresponds to the solar UV/EUV variations (Tsuchiya et al., 2011). However, the effect of solar UV/EUV heating on the brightness distribution of JSR has not been confirmed. Hence, the purpose of this study is to confirm the solar UV/EUV heating effect on total flux density and brightness distribution simultaneously, so as to evaluate the B-M scenario. In order to accomplish this purpose, we have made radio imaging analysis using the National Radio Astronomy Observatory (NRAO) archived data with the Very Large Array (VLA) obtained for about 10 days from January to February, 2000. We derived the total flux density and the dawn-dusk peak emission ratio of JSR and examined their relationship to the variation of the solar UV/EUV flux. From the VLA data analysis, following results were shown.

1, Total flux density variations occurred corresponding to the solar UV/EUV variations.
2, The dawn side emission was brighter than dusk side emission almost every day.
3, Variations of the dawn-dusk asymmetry did not correspond to the solar UV/EUV variations.

When we see a dawn-dusk ratio at the long term view (a week order), the second result supports the B-M scenario. However, from the third result, the observed variation feature of the dawn-dusk ratio cannot be examined solely by the solar UV/EUV heating. There is a possibility that variations related to the solar UV/EUV were masked by some other processes which dominated in the variations of the dawn-dusk ratio on the short time scale (day-order).

In order to explain the general features of the dawn-dusk ratio (the second result), we estimate the diurnal wind velocity from the observed dawn-dusk ratio by using the model brightness distribution of JSR. We construct the equatorial brightness distribution model and obtain the relation between the dawn-dusk ratio and neutral wind velocity. Estimated neutral wind velocity is 46 +/- 11 m/s, which reasonably corresponds to the numerical simulation of Jupiter's upper atmosphere (Tao et al., 2009). In order to explain short term variations of the dawn-dusk ratio (the third result), we examined the effect of the global convection electric field driven by tailward outflow of plasma in Jupiter's magnetosphere. As the result, it is suggested that typical fluctuation of the convection electric field strength was enough to cause the observed variations of the dawn-dusk ratio. It is also confirmed that some magnetospheric plasma parameters indicated the existence of substorm like event during the observation period. Hence, these results imply that fluctuations of tailward outflow affect Jupiter's deep inner magnetosphere.

Reference

Brice, N. M. and T. R. McDonough, Icarus, 18, 206-219, 1973.
Tao, C. et al., J. Geophys. Res., 114, A8, 2009.
Tsuchiya, F. et al., J. Geophys. Res., 116, A09202, 2011.

Keywords: Jupiter, Magnetosphere, Radiation Belt, Synchrotron Radiation, Radio Interferometer

Japan Geoscience Union Meeting 2012
(May 20-25 2012 at Makuhari, Chiba, Japan)

PCG33-14 Room:202 Time:May 25 14:30-14:45

Ground based multispectral imaging observation of Saturn's large storm

HAMAMOTO, Ko[1], TAKAHASHI, Yukihiro[1*], Makoto Watanabe[1], WATANABE, Shigeto[1], FUKUHARA, Tetsuya[1], SATO, Mitsuteru[1]

[1]Department of Cosmosciences, Graduate School of Science, Hokkaido University

Storms occur regularly in Saturn's atmosphere. Large storms called as Great White Spots(GWSs), which are about ten times larger than regular storms (300-3000 km in diameter), and occur about once per Saturnian year (29.5 Earth years). It is difficult to observe deep Saturn's atmosphere directly because Saturn's surface layer is covered by optically thick clouds. Observation of GWSs is one of the few method to get information about convective activity of Saturn's deep atmosphere [Hueso and Sanchez-Lavega, 2004]. In early studies, cloud structure of GWSs was estimated by radiative transfer calculation using images at several wavelengths in methane absorption bands [Acarreta and Sanchez-Lavega, 1999]. However, paucity of wavelengths in methane band have possibility to lead to ill-constrained cloud model parameters.

A new storm was detected on 5 December 2010, earlier than expected timing inferred from previous storm period by about ten years. The storm happened as a visible bright spot on northern hemisphere of Saturn (northern latitude of 37.7 degrees), and two weeks later, it's west-east size expanded 15,000 km. About two months after, it encircled the planet. This storm was observed by Cassini spacecraft. Cassini's images using three narrow bandpass filters (center wavelengths are 727, 750, 889 nm) showed horizontal variation of brightness at these wavelengths [Fischer et al., 2011]. However, the detail spectral information of the storm is still unknown. And also there is no comparison of spectrums in different periods.

In this study, an observation of the Saturn's storm used Multi-Spectral Imager(MSI) and a ground-based 1.6 m reflector named Pirka telescope operated by Hokkdaido University. MSI, which uses two Liquid Crystal Tunable Filters(LCTF) and an EM-CCD, was developed in Hokkaido University and enabled us to capture spectral images in a short time. Spectral imaging data of the storm, in the wavelength range of 400-1100 nm with FWHM of 5-10 nm, at 180 colors, were obtained within 30 minutes on 5 May 2011. Additionally on 6 June 2011, we observe Saturn in three methane bands at 88 colors.

We succeeded in deriving latitudinal variation of Saturn's spectrum in visible and near-infrared range. Methane absorption bands were confirmed and the rough shape of the spectrum is consistent with past observations [ex. Karkoschka, 1994]. And center-limb profile of spectrum at same latitude have possibility to provide characteristic of scattering, because of less longitudinal variation of spectrum.In addition, we drew a comparison between latitudinal variation of Saturn's absolute reflectivity in three methane absorption bands on 5 May and 6 June. In these datas, the reflectivity slightly changed In about a month. This period is fading phase of this GWS. Therefore detection of an absolute reflectivity variation at the latitude of the GWS lead to a fading speed information of the GWS. And a reflectivity of Saturn after the GWS fade outed is also important in terms of an influence on static cloud level by the GWS. Therefore, we are scheduled to observe Saturn in spring of 2012.

In future works we will observe Saturn's atmosphere regularly to derive temporal variation of spectrums and cloud structure using Pirka telescope.

Keywords: Saturn, great white spot, ground based observation, spectrum

Japan Geoscience Union Meeting 2012
(May 20-25 2012 at Makuhari, Chiba, Japan)

PCG33-15 Room:202 Time:May 25 14:45-15:00

De effect on Jupiter's decametric non-Io-A source

IMAI, Kazumasa[1*], FUKUSHIMA, Koichi[1], UJIHARA, Akiya[1], IMAI, Masafumi[2]

[1]Department of Electrical Engineering and Information Science, Kochi National College of Technology, [2]Department of Geophysics, Graduate School of Kyoto University

One of the unresolved problems of Jupiter's decametric radio emissions is the variation of occurrence probability on the order of a decade. The variation was first thought to be due to changes in solar activity (solar cycle). The Sun can influence the detection of Jovian decametric radiation by changing the local observing conditions, changing the density of plasma in the interplanetary medium and by changing conditions at the Jupiter radio source.

The period of the variation was also close to the orbital period of Jupiter (11.86 years). Carr et al. [1970] showed that such variations are closely correlated with the Jovicentric declination of the Earth (De). The range of the smoothed variation of De is from approximately +3.3 to -3.3 degrees. If this is the case, the observed variation appears to be a purely geometric effect caused by changes in the beam cross section seen from the Earth. The shape and angular dimensions of the part of the emission beam accessible to the Earth is shown in Figure 6a in Carr et al. [1970]. However the detail of the beam model has not been proposed so far.

Garcia [1996] extensively studied and confirmed this De effect. The radio observations used in this study were mainly taken by Yagi antennas located at the University of Florida Radio Observatory (UFRO). The occurrence probability of the non-Io-A source varies in close step with De. Garcia [1996] reports that the changes in source width and location for non-Io-A are very large over the roughly 7 degree range of De. The high CML edge of the non-Io-A source also has a very strong dependence on De.

We show the long-term periodic variation of the occurrence probability of Jupiter's decametric radio emissions is caused by the De effect which is related to the pure geometrical effect of sharp radio beaming. We propose the searchlight beam model which can explain this sharp beaming especially in a latitudinal direction. The three dimensional structure of the radio source is the important key parameter to produce the searchlight beam of Jupiter's decametric radio emissions. We calculate the beam pattern by using the dimensions of the radio coherent region. The calculated results show the existence of sharp beaming in the latitudinal direction. As the searchlight beam is the intensified part of a conical sheet beaming toward the equatorial plane, it does not conflict with the previous idea of the conical sheet model. We also propose the delta zone effect to explain the cyclic changes of CML and the effective width of the non-Io-A source. We believe that the searchlight beam model is very important in understanding the beaming of the planetary radio emissions.

References

Carr, T.D., A.G. Smith, F.F. Donivan, and H.I. Register, The twelve-year periodicities of the decametric radiation of Jupiter, Radio Sci., 5, pp.495-503, 1970.

Imai, K., L. Garcia, F. Reyes, M. Imai, and J.R. Thieman, A Model of Jupiter's decametric Radio emissions as a searchlight beam, Planetary Radio Emissions VII, edited by H.O. Rucker, W.S. Kurth, P. Louarn, and G. Fischer, Austrian Academy of Sciences, Graz, Austria, pp.179-186, 2011.

Keywords: Jupiter Radio, decametric wave, beam structure, De effect, radio source, radio emission mechanism